Model Based Detection of Branching Structures

Li Wang and Abhir Bhalerao*
University of Warwick, Coventry, CV4 7AL, UK

Abstract. This paper presents a method for modelling and estimating 2D or 3D branching structures, such as blood vessel bifurcations from medical images. Branches are modelled as a superposition of Gaussian functions in a local region which describe the amplitude, position and orientations of intersecting linear features. The centroids of component features are separated by applying K-means to the local Fourier phase and the covariances and amplitudes subsequently estimated by a likelihood maximisation. A penalised likelihood test, the Akakie Information Criteria (AIC), is employed to select the best fit model in a region. Experimental results are presented on 2D retinal images and synthetic 3D data.

1 Introduction

The detection of line, corner and branching structures is a widely studied problem in computer vision, especially for object recognition, and is an important one for tasks such as image registration and segmentation in medical imaging. In this work, our aim is to derive a reliable method for the quantisation of branching structures from 2D and 3D medical imagery and apply it to problems such as segmenting the blood vessels from retinal images [1], and characterising the bronchial tree from 3D CT images [2].

Broadly speaking, corner detection techniques can be classified into two major categories: geometry-based and template-based. For geometry-based approaches, many of the algorithms use gradient information to locate corner position. Methods that use the intersections of boundaries to label corners necessitate the thinning of curves to a single pixel width e.g. by skeletonisation. Because of ambiguities caused by the line thinning, the subsequent labelling of branch points can be problematic, particularly in 3D. In general, methods that depends on the second or greater order differentials of the image intensity are sensitive to noise, whereas template approaches are limited in the range and type of branch points that can be described [3]. Scale-space curvature algorithm provides some trade-off between these approaches because of the noise immunity gained by repeated smoothing, plus the ability to naturally model the size of features and, by tracking curvature through scale, allowing labelling decisions to be confirmed by comparing estimates at different scales in the feature space. The disadvantages are computational expensive and not readily extend to 3D [4].

We propose a model based estimation that operates directly on the image intensities. Regions of the image are modelled locally as a superposition of M Gaussian functions and an iterative, ML estimation used to derive the parameters. Each Gaussian represents a single, approximately linear feature in the region which parameterised by a mean (centroid), an orientation and width (covariance), and an amplitude. Models for $M = 1, 2$ are fitted separately to the region and a penalised likelihood information measure, the Akakie Information Criterion (AIC), is used to choose the best for a given region size. The feature parameters are first separated using K-means by modelling the local phase-spectrum, which is linearly dependent on the component centroids. Having established an initial estimate of the component centroids, the feature covariances and amplitudes are estimated by a weighted maximisation that has similarities to EM. After a description of the model and estimation algorithms, results are presented on a sample retinal fundus image and synthetic 3D data. We conclude by a discussion of the results and make some proposals for further work.

2 Branch Feature Modelling and Selection

In the spatial frequency domain, multiple linear features within the same region (Figure 1(d)) are modelled as a superposition of Gaussian models and the spectrum is approximated as a sum of component spectra:

$$G(\vec{\omega}) = \sum_{m=1}^{M} |G_m(\vec{\omega})| \exp[-j\phi_m(\vec{\omega})] \tag{1}$$

where $G_m()$ is the mth Gaussian feature and $\phi_m()$ is the corresponding phase spectrum. In particular, the phase-spectrum of a component exhibits a phase variation which is dependent on the feature centroid and the spectral

*Email: {liwang, abhir}@dcs.warwick.ac.uk

energy is concentrated in a direction orthogonal to the spatial orientation. We assume that this phase variation is independent for each of the M components of the model [5]:

$$\phi(\vec{\omega}) = \sum_{m=1}^{M} \phi_m(\vec{\omega}_m) = -\frac{B}{2\pi} \sum_{m=1}^{M} \vec{\mu}_m \cdot \vec{\omega}_m, \qquad T_m = \frac{1}{||\Omega_m||} \sum_{\vec{\omega} \in \Omega_m} \frac{\vec{\omega}\vec{\omega}^T |G(\vec{\omega})|}{||\vec{\omega}||} \tag{2}$$

Feature components are estimated by first separating out the component centroids using K-means clustering. At each step of the clustering, the phase-spectrum of each component is reconstructed using the current estimate of its centroid starting with M random positions. Each spatial frequency coordinate of the data phase-spectrum is then assigned to the closest component value and the new centroid estimates calculated from these partitions, Ω_m. The process is repeated until the centroid positions stabilise (typically $<$10 iterations). The M spatial frequency coordinate partitions are subsequently used to estimate the orientations of the Gaussian components. By forming tensors T_m, an estimate can be made of the component covariances, C_m. Performing PCA on T yields the principal axes of the features forming the branch point and the corresponding eigen values are the widths (as variances).

This Fourier based estimation is computationally efficient and accurate in noise free data but can be greatly improved against noise by maximising the inner product between the windowed data, $f_B()$, and the model, G:

$$\arg_\Theta \max \sum_{\vec{x}} f_B(\vec{x}) G_m(\vec{x}|\Theta) \tag{3}$$

The result is a set of iterative equations that calculate sample statistics weighted by $w^t(\vec{x}) = f_B(\vec{x}) G_m(\vec{x}|\Theta_t)$ that are similar to the expectation step of EM. Unlike EM however, the weights here are not probabilities and do not sum to 1. More importantly, the estimation implicitly takes into account the spatial arrangement of the data $f_B(\vec{x})$ relative to the intensity model $G(\vec{x})$ whereas EM estimates the underlying distribution from which $f_B(\vec{x})$ are drawn. For each feature m in the window, the parametric set Θ_{t+1} can be calculated by:

$$A_m^{t+1} = \sum_{\vec{x}} w^t(\vec{x}) / \sum_{\vec{x}} G^2{}_m(\vec{x}|\Theta_t), \qquad \vec{\mu}_m^{t+1} = \sum_{\vec{x}} w^t(\vec{x})\vec{x} / \sum_{\vec{x}} w^t(\vec{x})$$
$$C_m^{t+1} = 2 \sum_{\vec{x}} w^t(\vec{x})(\vec{x} - \vec{\mu}_t)(\vec{x} - \vec{\mu}_t)^T / \sum_{\vec{x}} w^t(\vec{x}) \tag{4}$$

where t denotes iteration number and Θ_0 is the estimate from the spectrum of $f_B()$ using Eqn: 2. Convergence is achieved rapidly in 3-5 iterations. Figure 1 shows estimates of two type of linear features in part of a 2D retinal angiographic image for single and multiple Gaussian models.

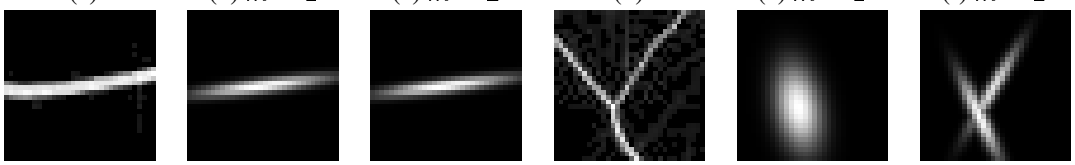

Figure 1. (a)-(c): Estimation of a linear structure shown in (a) using single and multiple Gaussian intensity models (b),(c). (d)-(f): Estimation of branching structure shown in (d) using single and multiple models (e),(f). Block size is 32×32.

Since we have multiple feature models, $m = 1, 2$, once the parameters of each model have been estimated, the accuracy of the hypothesis and the most fit model needs be determined in order to represent a given image region. We use a penalised distance measure, the Akaike information criterion (AIC), to bias the residual fit error which is expected to fall with increasing m. In minimum mean-square estimation, AIC is calculated using residual sums of squares (RSS)

$$AIC_m = B^n \, ln(RSS/B^n) + 2P \tag{5}$$

where B^n is the number of data points in a square image region size B and P is the number of parameters in the model. The steps to finding the optimal model m_{opt} is summarised below:

1. Estimate the initial parameters for each model $m = 1..M$ for some block size B.
2. Use Eqns. 4 to improve the first estimate for each model m.
3. Compute AIC_m from RSS_m.
4. Repeat steps $(1) - (3)$ for $m + 1 \leq M$ (Eq. 5).
5. $m_{opt} = \arg_m \min(AIC_m)$.

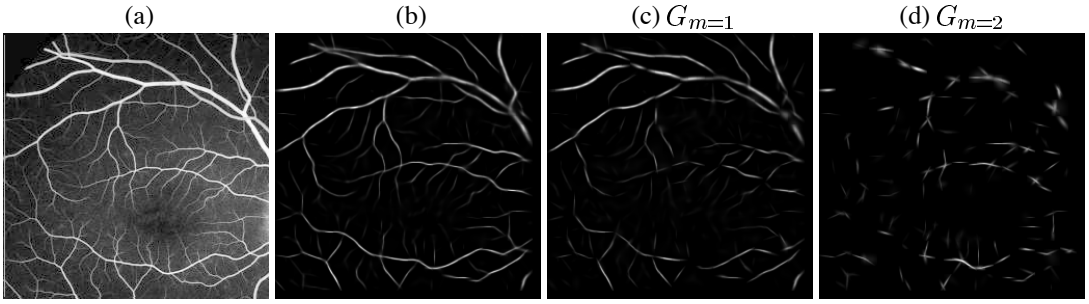

Figure 2. (a) Part of human retinal angiographic image. (b) Multiple Gaussian model reconstructions (c) Reconstructions showing only single Gaussian model selections, $m = 1$. (d) Reconstructions showing only multiple Gaussian model selections, $m = 2$. (Block sizes 16×16).

3 Experiments and Discussion

The results of the ML model estimation and selection algorithm were tested by using a retinal image size 256×256, shown in figure 2(a). Figure 2b shows reconstructions of the data using multiple feature model. Overall, after the iterative ML estimation, the orientation, position and width of the features both along blood vessels and near bifurcations are accurately modelled. Based on the AIC selection scheme, we then attempted to select the best fit model, $m = 1, 2$, for each block and produced the data reconstruction shown in figure 2(c)-(d). Junction points are localised to regions where $G_{m=2}$ is optimal. The feature intersection point can be trivially calculated from the model parameters, $\Theta_{m=1,2}$, in these blocks. In figure 3(a)-(b), the regions containing an inferred junction point or point of high curvature are highlighted by drawing a circle centred on the intersection and with the radius $B/2$ to indicate the detection scale.

By means of comparison, we implemented a popular curvature scale-space method (from Lindeberg [4]) which has been widely used on edge or corner detections problem in computer vision. Under this representation,the corner is detected by measuring the curvature of level curves, R, i.e. the change of gradient direction along an edge contour:

$$R = S^2_{x_2} S_{x_1^2} - 2 S_{x_1} S_{x_2} S_{x_1 x_2} + S^2_{x_1} S_{x_2^2} \tag{6}$$

where S_{x_i} is the convolution between the original image and Gaussian kernels of different variance. In one variation of this approach, as used here to produce Figure 3(c)-(d), the curvature is further multiplied by the gradient magnitude raised to the third power.

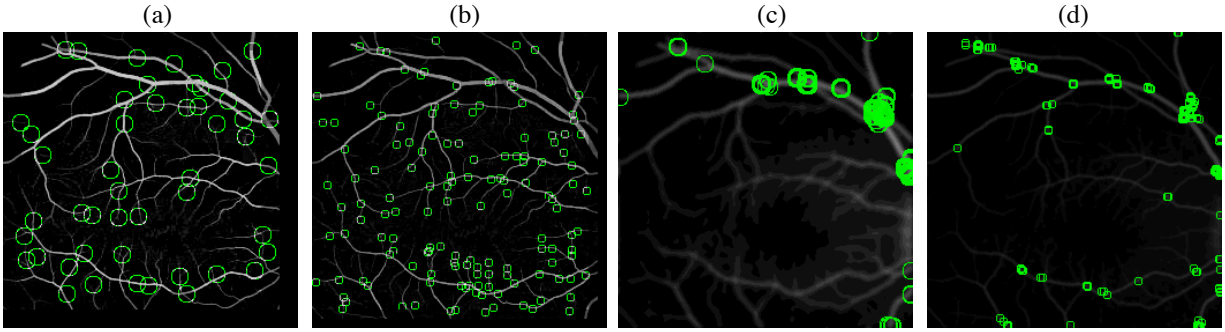

Figure 3. (a)-(b) Branch point candidates labelled after model selection at block sizes 32×32 and 16×16.(c)-(d) The 150 strongest corner responses of R from curvature scale-space representation at equivalent scales. (The radii of the circles reflect the detection scales).

	No. of Junctions	*False-positive*	*False-negative*
Manual	65	0	0
Gaussian Model	60	80	5
Scale-space ($t = 0.1, 0.5, 1$)	32	118	33

Table 1. Results of validation with manual counting at one scale (16×16).

Comparing the results given in figure 3 we observe that using the Gaussian model a greater number of the junction points or corners are detected than by the scale-space curvature. The scale-space method fails to find many of the

branches at small scales, although this could be perhaps improved by parameter tuning. We attempted to validate our detector by noting the numbers of false-positive and false-negative labellings compared with a visual inspection and the curvature scale-space method, table 1. Our estimator produces some failures (mostly false-positives) in the retinal image but compares well with the scale-space results. Also like the curvature scale-space, it does not distinguish between true junctions and points of high curvature (corners). In terms of computational efficiency, our estimator is approximately equivalent to a pair of 9×9 spatial convolution operators, which is an order or magnitude better than a curvature scale-space implementation.

Using the same algorithm but adding an additional dimension, we also implemented it on a 3D synthetic tree-structure image, which is shown in figure 4. Figure 4(b) shows the model reconstruction result at block size $16 \times 16 \times 16$. Branch structures are well represented using multiple feature model and after the model selection scheme, blocks which contain junction candidates are highlighted in figure 4(c).

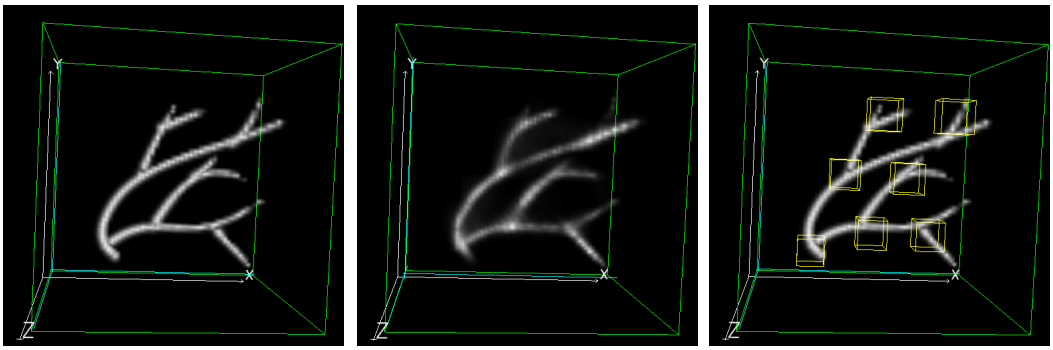

(a) (b) (c)

Figure 4. (a) Synthetic 3D tree-Structure date ($64 \times 64 \times 64$) (b) Multiple feature reconstruction with block size $16 \times 16 \times 16$ (c) Blocks which contain branching points candidates (Size of the cube reflect detection level)

4 Conclusions

We have described a modelling and estimation method that uses a superposition of Gaussian functions to model the local image intensity. The methods can be usefully applied to the detection and quantification of tree-like structures in medical images. The estimator is cheap to compute and robust in the presence of uncertainties in the image due to low signal to noise ratios and our preliminary results seem to compare favourably with curvature scale-space approaches, although objective validation is necessary. The illustrative results of the image modelling show it to work well for linear structures in 2D and 3D images. Work toward a complete segmentation of the image will need a neighbourhood linking strategy to track features from region to region, perhaps within a Bayesian framework [6].

5 Acknowledgements

The authors gratefully acknowledge UK EPSRC (GR/M82899/01) for funding this work.

References

1. M. E. Martinez-Perez, A. D. Hughes, A. V. Stanton et al. "Retinal blood vessel segmentation by means of scale-space analysis and region growing." In *Proceedings of the International Conference on Image Processing*, volume 2, pp. 173–176. 1999.
2. V. Sauret, K. A. Goatman, J. S. Fleming et al. "Semi-automated tabulation if the 3d topology and morphology of branching networks using CT: Application to the airway tree." In *Phys. Med. Biol*, p. 44. 1999.
3. R. Mehrotr, S. Nichani & N. Ranganathan. "Corner detection." *Pattern Recognition* **23(11)**, pp. 1223–1233, 1990.
4. T. Lindeberg. "Junction detection with automatic selection of detection scales and localization scales." In *Proc. 1st International Conference on Image Processing*, volume 1, pp. 924–928. Nov. 1994.
5. A. R. Davies & R. Wilson. "Curve and corner extraction using the multiresolution fourier transform." In *Image Processing and its Applications*. 4h IEE Conf., 1992.
6. A. Bhalerao, E. Thönnes, W. Kendall et al. "Inferring vascular structure from 2d and 3d imagery." In *Medical Image Computing and Computer-Assisted Intervention*. 2001.